

Magnetic properties of Fe-Ni-system films prepared by electroless deposition

Cite as: AIP Advances **10**, 015047 (2020); <https://doi.org/10.1063/1.5130446>

Submitted: 19 October 2019 . Accepted: 16 December 2019 . Published Online: 22 January 2020

Takeshi Yanai, Ryoma Tanaka, Ryoya Ueno, Kafu Mieda, Junichi Kaji, Takao Morimura, Akihiro Yamashita, Masaki Nakano , and Hirotohi Fukunaga

COLLECTIONS

Paper published as part of the special topic on [64th Annual Conference on Magnetism and Magnetic Materials](#)

Note: This paper was presented at the 64th Annual Conference on Magnetism and Magnetic Materials.



View Online



Export Citation



CrossMark

ARTICLES YOU MAY BE INTERESTED IN

[Direct writing of room temperature and zero field skyrmion lattices by a scanning local magnetic field](#)

Applied Physics Letters **112**, 132405 (2018); <https://doi.org/10.1063/1.5021172>


[Design of an erasable spintronics memory based on current-path-dependent field-free spin orbit torque](#)

AIP Advances **10**, 015317 (2020); <https://doi.org/10.1063/1.5130050>

[Single crystalline boron rich B\(Al\)N alloys grown by MOVPE](#)

Applied Physics Letters **116**, 042101 (2020); <https://doi.org/10.1063/1.5135505>



NEW



AVS Quantum Science

A new interdisciplinary home for impactful quantum science research and reviews

Co-Published by

NOW ONLINE



Magnetic properties of Fe-Ni-system films prepared by electroless deposition

Cite as: AIP Advances 10, 015047 (2020); doi: 10.1063/1.5130446
Presented: 6 November 2019 • Submitted: 19 October 2019 •
Accepted: 16 December 2019 • Published Online: 22 January 2020



Takeshi Yanai, Ryoma Tanaka,^{a)} Ryoya Ueno, Kafu Mieda, Junichi Kaji, Takao Morimura, Akihiro Yamashita, Masaki Nakano,^{id} and Hirotooshi Fukunaga

AFFILIATIONS

Nagasaki University, 1-14 Bunkyo-machi, Nagasaki 852-8521, Japan

Note: This paper was presented at the 64th Annual Conference on Magnetism and Magnetic Materials.

^{a)}e-mail: bb52119228@ms.nagasaki-u.ac.jp

ABSTRACT

We prepared Fe-Ni thick-films ($> 1 \mu\text{m}$) using an electroless deposition method and evaluated the magnetic properties and the crystal structures. The deposition rate depended on the concentration of dimethylamine-borane (DMAB), which is a reducing agent used in the present study, and we obtained a high deposition rate ($> 10 \mu\text{m/h}$) for $\text{Fe}_{30}\text{Ni}_{70}$ films when the DMAB concentration is higher than 3 g/L. From structural analyses of the films, we found that the films have very fine fcc Fe-Ni crystals in the amorphous magnetic phase. From the investigation of Co additives for the improvement in the surface conditions, we confirmed that a small amount of Co effectively works to obtain the smooth surfaces. As a result, we could obtain the Fe-Ni-system thick-films with low coercivity (50 A/m) and smooth surfaces.

© 2020 Author(s). All article content, except where otherwise noted, is licensed under a Creative Commons Attribution (CC BY) license (<http://creativecommons.org/licenses/by/4.0/>). <https://doi.org/10.1063/1.5130446>

I. INTRODUCTION

In recent years, driving-frequency of electric devices has increased for improvement in their performance, and the development of magnetic devices, which can be used under a high frequency, is strongly required. For high-frequency driving of magnetic materials in the devices, we need to reduce eddy current losses, and one of the effective methods to reduce the loss is a reduction in the thickness. Fe-Ni alloys are well-known as a superior soft magnetic material owing to their low coercivity and high permeability, and film-shaped Fe-Ni alloys are preferable to operate under a high frequency. Various fabrication processes of soft magnetic films have been reported, and electrodeposition techniques are one of the popular methods to obtain Fe-Ni films¹⁻⁵ due to their high deposition rates.

Electroless deposition is also attractive methods since they have high selectivity of substrates and high uniformity of film thickness.^{6,7} In fact, electroless deposition of Ni films is widely used in the industrial field. Focusing on the fabrication of Fe-Ni films using electroless deposition methods, some researchers have reported the films using dimethylamine borane (DMAB) as a reducing agent.⁸⁻¹⁰ Although good soft magnetic properties have been reported for electroless-deposited Fe-Ni films, the deposition rate is not high

($< 10 \mu\text{m/h}$) and discussion about the magnetic properties for Fe-Ni thick-films ($> 5 \mu\text{m}$) was not enough. In the present study, we, therefore, fabricated the Fe-Ni thick-films using an electroless deposition method and evaluated the magnetic properties and the crystal structure.

II. EXPERIMENTAL PROCEDURE

A. Electroless deposition

The plating bath conditions are shown in Table I. The DMAB was employed as a reducing agent, and its concentration was changed from 3 to 10 g/L. To evaluate the effect of Co addition on the surface conditions (related to Figs. 6-7), $\text{CoSO}_4 \cdot 7\text{H}_2\text{O}$ (Cobalt sulfate) was added by the replacement of $\text{NiSO}_4 \cdot 6\text{H}_2\text{O}$.

The electroless deposition conditions are summarized in Table II. In the present study, we employed Cu plates as substrates since we can directly obtain the Fe-Ni films (Fe < 45 at.%), indicating that we don't need an imparting catalyst process before the deposition. The pH of the bath was adjusted with KOH.

B. Measurements

The thickness and the surface roughness R_a of the as-deposited films were measured with a micrometer (Mitutoyo, CPM15-25M)

TABLE I. Bath conditions.

Components	Concentration
NiSO ₄ ·6H ₂ O (Nickel sulfate)	50 - x [g/L]
FeSO ₄ ·7H ₂ O (Iron sulfate)	70 g/L
CoSO ₄ ·7H ₂ O (Cobalt sulfate)	x = 0 - 40 g/L
Na ₃ C ₆ H ₅ O ₇ ·2H ₂ O (Tri-Sodium citrate)	110 g/L
(NH ₄) ₂ SO ₄ (Ammonium sulfate)	60 g/L
NH ₄ NH ₂ SO ₃ (Ammonium amid sulfate)	25 g/L
H ₃ BO ₃ (Boric acid)	25 g/L
(CH ₃) ₂ NH·BH ₃ (DMAB)	3-10 g/L

TABLE II. Electroless deposition conditions.

Conditions	Value
Bath temperature	85°C
Substrate	Cu (thickness 500 μm)
Deposition area	25 mm × 5 mm
Deposition time	5 - 60 min
pH	7.5

and a surface roughness meter (Mitutoyo, Surf Test SV-400), respectively. We evaluated the coercivity from the dc B-H loops ($f = 50$ mHz) using a B-H curve tracer (Riken Denshi, BHS-40). The film composition and the microstructure were analyzed by an energy dispersive X-ray spectrometry (Hitachi High-technologies S-3000) and a transmission electron microscope observation (JEOL, JEM-2010), respectively. Thermomagnetic curve and X-ray diffraction pattern (Rigaku, Miniflex600-DX) were used to discuss magnetic phases in the film and the change in the structure over the composition, respectively.

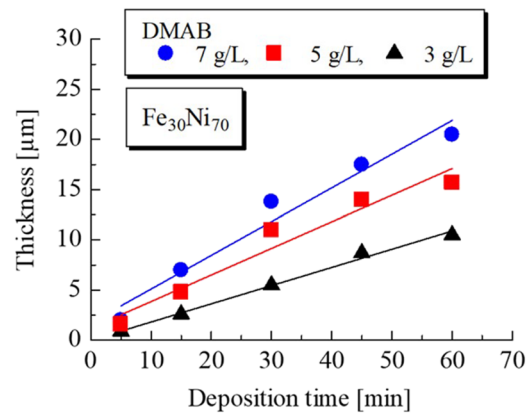
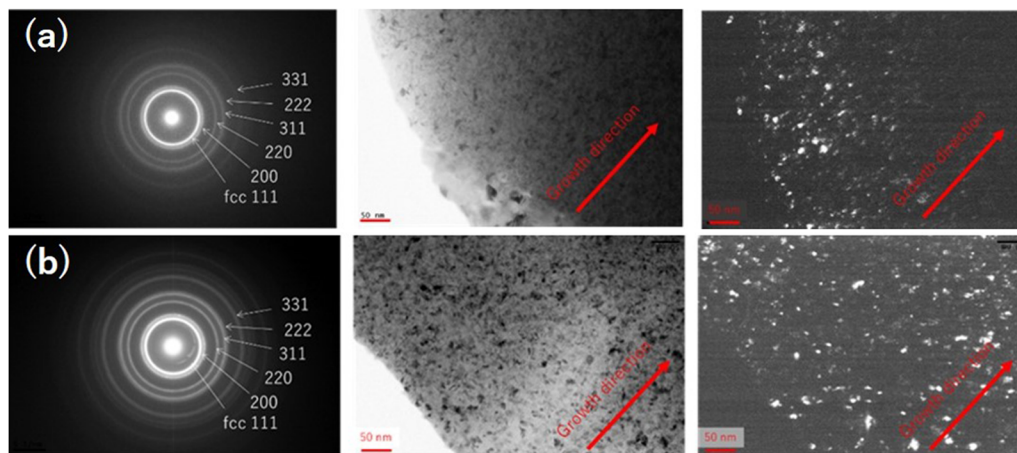


FIG. 1. Thicknesses of the Fe-Ni films as a function of the deposition time.

III. RESULTS AND DISCUSSION

Figure 1 shows the thickness of the Fe₃₀Ni₇₀ films as a function of the deposition time. The results for the DMAB concentrations of 3, 5, and 7 g/L are shown in Fig. 1. The thickness increased with increasing the deposition time, and we confirmed that much thicker films could be obtained by the increase in the DMAB concentrations. The deposition rate for 7 g/L is approximately 20 μm/h, and this value is higher than that of Ref. 9.

To confirm the film structures, we evaluated the microstructure using TEM. Figure 2 shows TEM images of the Fe₃₀Ni₇₀ film (FeSO₄: 70 g/L) and the Fe₄₅Ni₅₅ one (FeSO₄: 90 g/L). The obtained diffraction pattern could be indexed as an fcc Fe-Ni, and the bright and dark field images imply that the films have very fine structures. Figure 3 shows the thermal magnetization curve of the Fe₃₀Ni₇₀ film. As shown in Fig. 3, we confirmed two Curie points, and the higher point (approx. 600°C) is attributed to the fcc Fe-Ni crystalline phase. Since only the fcc Fe-Ni crystalline phase was confirmed in the diffraction pattern of the TEM observation, we considered that the lower Curie point (approx. 300°C) is attributed to an amorphous

FIG. 2. Electron diffraction pattern, and bright and dark-field TEM images of (a) the Fe₃₀Ni₇₀ film and (b) the Fe₄₅Ni₅₅ one prepared at the DMAB concentration of 5 g/L.

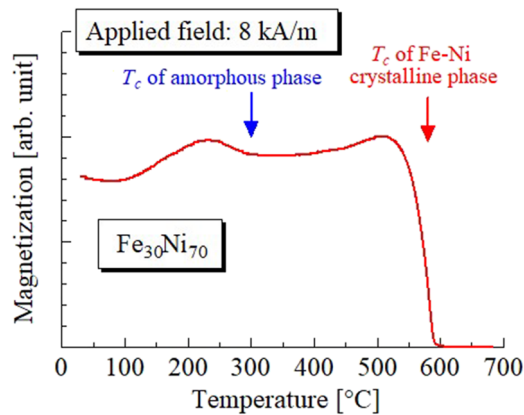


FIG. 3. Thermal magnetization curve of the $\text{Fe}_{30}\text{Ni}_{70}$ film.

magnetic phase. From the structural analysis, we found that the fcc nanocrystals exist in the amorphous matrix phase. As the boron in the DMAB is incorporated into the Fe-Ni films,⁸ we considered that the small amount of the boron effectively worked to obtain the fine structures.

It is well-known for nanocrystalline soft magnetic materials that the reduction in the grain size is effective to improve the soft magnetic properties.¹¹ As our films have very small grains as mentioned above, superior soft magnetic properties are expected. To confirm the soft magnetic properties, we evaluated the coercivity of the $\text{Fe}_{30}\text{Ni}_{70}$ films as a function of the DMAB concentration and the result is shown in Fig. 4. The evaluated result of the surface roughness R_a is also shown in Fig. 4. As shown in Fig. 4, both H_c and R_a increased with increasing the DMAB concentration. Figure 5 shows the SEM images of the surface for the films prepared at the DMAB concentration of 5 and 10 g/L. The surface for 10 g/L was obviously rough compared with that for 5 g/L. For soft magnetic materials, as the surface roughness is one of the factors to determine their magnetic properties, we need to improve the surface conditions to obtain good soft magnetic properties.

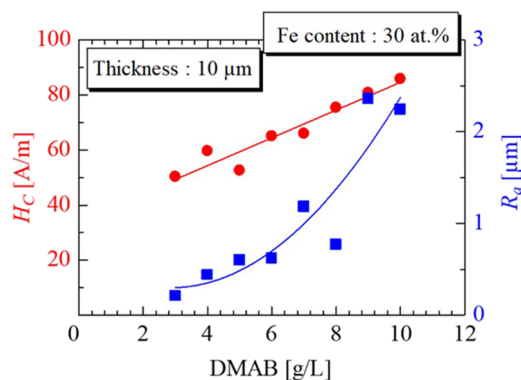


FIG. 4. The coercivity H_c and the surface roughness R_a of the $\text{Fe}_{30}\text{Ni}_{70}$ films as a function of the DMAB concentration.

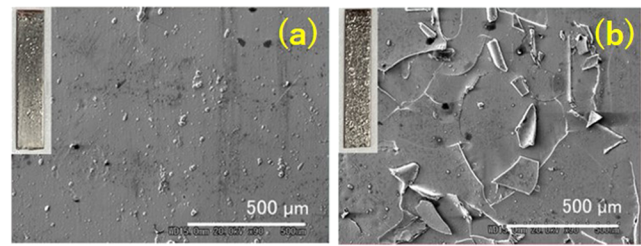


FIG. 5. SEM images of the $\text{Fe}_{30}\text{Ni}_{70}$ films prepared at the DMAB concentration of (a) 5 and (b) 10 g/L.

As shown in Fig. 4, the decrease in the DMAB concentration is effective to improve surface conditions. However, high DMAB concentration is important to obtain a high deposition rate, and we, therefore, investigated Co additives as another improvement method of the surface. Since the standard electrode potential of Co^{2+} is less than that of Ni^{2+} , the slight reduction in the reducing rate is expected.¹² Consequently, we expected the improvement in the surface roughness by the partial replace of Ni to Co in the Fe-Ni films.

Figure 6 shows the coercivity H_c and the surface roughness R_a as a function of the Co content of the films. In this experiment, the DMAB concentration was fixed at 5 g/L and the thickness was adjusted at 5 μm . As shown in Fig. 6, H_c dramatically increased when the Co content was higher than 30 at.%, and R_a decreased with increasing the Co content. Figure 7 shows the SEM images of the surface of $\text{Fe}_{30}\text{Ni}_{50}\text{Co}_{20}$ film and $\text{Fe}_{30}\text{Ni}_{30}\text{Co}_{40}$ one. Compared with Fe-Ni films in Fig. 5 (b), we confirmed that the Co additive improves the surface conditions.

As discussed in Fig. 4, low R_a is one of the factors to obtain low coercivity. The $\text{Fe}_{30}\text{Ni}_{30}\text{Co}_{40}$ film in Fig. 6 did not show low coercivity despite low R_a . This result implies that another factor increases the coercivity. To clarify the reason for the high coercivity of the $\text{Fe}_{30}\text{Ni}_{30}\text{Co}_{40}$ film, we evaluated the structures of the films using X-ray diffraction patterns. Figure 8 shows the XRD patterns of $\text{Fe}_{30}\text{Ni}_{70-x}\text{Co}_x$ films. The diffraction peaks of the films with $x < 25$ were identified as the fcc Fe-Ni crystalline phase. In high

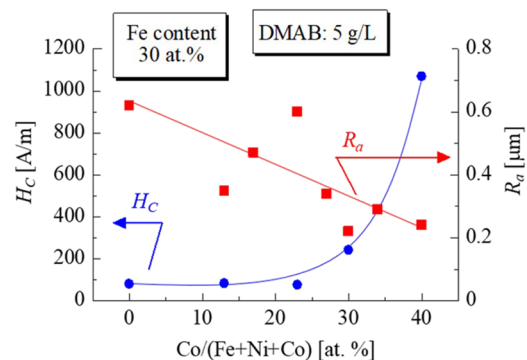


FIG. 6. The coercivity H_c and the surface roughness R_a as a function of the Co content of the Fe-Ni-Co films.

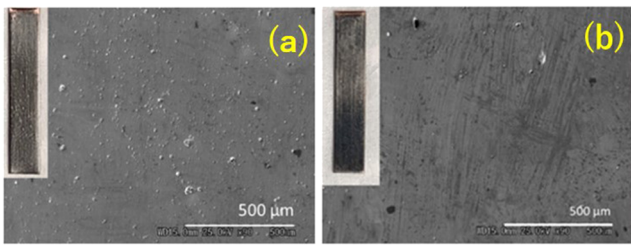


FIG. 7. SEM images of the surface of the (a) $\text{Fe}_{30}\text{Ni}_{50}\text{Co}_{70}$ film and (b) the $\text{Fe}_{30}\text{-Ni}_{30}\text{-Co}_{40}$ film.

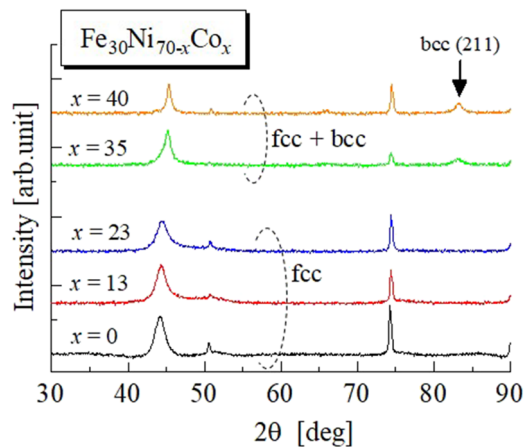


FIG. 8. X-ray diffraction patterns of $\text{Fe}_{30}\text{Ni}_{70-x}\text{Co}_x$ films.

Co content films, the diffraction peak of bcc (211) was observed together with the peaks of fcc. In our experimental conditions, the bcc structure was observed when the Co content is higher than 30 at.%. As shown in Fig. 6, the coercivity dramatically increased around the Co content of approximately 30 at.%. Therefore, we consider that the effect of the structural change (formation of the bcc structure) is much stronger than that of the reduction in R_d on the coercivity.

From these results, we found that a small amount of Co (< 20 at.%) is effective in improving the surface condition of the electroless deposited Fe-Ni films without deterioration of good soft magnetic properties.

IV. CONCLUSION

We investigated the structure and the magnetic properties of the Fe-Ni-system films prepared by the electroless deposition method. The obtained results are summarized as follows:

- (1) The increase in the concentration of DMAB increases the deposition rate, and we obtained a high deposition rate (> 10 $\mu\text{m/h}$).
- (2) The grain with the amorphous matrix phase was very fine (< 10 nm).
- (3) One of the factors to increase the coercivity was rough surface, and a small amount of Co was effective in improving the surface condition keeping good soft magnetic properties.

REFERENCES

- ¹T. Osaka, M. Takai, K. Hayashi, K. Ohashi, M. Saito, and K. Yamada, "A softmagnetic CoNiFe film with high saturation magnetic flux density and low coercivity," *Letters to Nature* **392**, 796 (1998).
- ²H.-S. Nam, T. Yokoshima, T. Nakanishi, T. Osaka, Y. Yamazaki, and D. N. Lee, "Microstructure of electroplated soft magnetic CoNiFe thin films," *Thin Solid Films* **384**, 288 (2001).
- ³T. Liu, Z. Lu, D. Li, L. I. Peng, Y. Lu, K. Sun, and S. Zhou, "Influence of electroplating conditions on magnetic properties of Fe-36 wt. % Ni alloy film," *Rare Metals* **25**, 484 (2006).
- ⁴X. W. Hou, S. B. Liu, S. L. Yang, J. Li, and B. Guo, "Electrical and magnetic properties of electrodeposited Fe-based alloys used for thin film transformer," *Science China* **56**, 84 (2013).
- ⁵M. Theis, S. Ediger, M. T. Schmitt, J.-E. Hoffmann, and M. Saumer, "Nanocrystalline electroplated NiFe-based alloys for integrated magnetic microsensors," *Physica Atatus Solidi A* **210**, 853 (2013).
- ⁶R. A. Belakhmimaa, N. Errahmánya, M. Ebn Touhamia, H. Larhzilab, and R. Tuir, "Preparation and characterization of electroless Cu-P deposition protection for mild steel corrosion in molar hydrochloric solution," *Journal of the Association of Arab Universities for Basic and Applied Sciences* **24**, 46 (2017).
- ⁷J. N. Balaraju, T. S. N. Sanakara Narayanan, and S. K. Seshadri, "Electroless Ni-P composite coating," *Journal of Applied Electrochemistry* **33**, 807 (2003).
- ⁸T. Yamamoto, T. Nagayama, and T. Nakamura, "Thermal expansion and thermal stress behavior of electroless-plated Fe-Ni-B alloy thin film for high-density packaging," *Journal of The Electrochemical Society* **166**, D3228 (2019).
- ⁹R. Anthony, B. J. Shanahan, F. Waldron, C. Mathuna, and J. F. Rohan, "Anisotropic Ni-Fe-B films with varying alloy composition for high frequency magnetics on silicon applications," *Applied Surface Science* **357**, 385 (2015).
- ¹⁰T. Yokoshima, D. Kaneko, M. Akahori, H. S. Nam, and T. Osaka, "Electroless CoNiFeB soft magnetic thin films with high corrosion resistance," *Journal of Electroanalytical Chemistry* **491**, 197 (2000).
- ¹¹G. Herzer, "Grain size dependence of coercivity and permeability in nanocrystalline ferromagnet," *IEEE Transactions on Magnetics* **25**, 1397 (1989).
- ¹²W. L. Liu, S. H. Hsieh, W. J. Chen, and Y. C. Hsu, "Growth behavior of electroless Ni-Co-P deposits on Fe," *Applied Surface Science* **255**, 3880 (2009).